

Constraining gravitational-wave polarizations with Taiji

Chang Liu^{1,2,*} Wen-Hong Ruan^{1,2,†} and Zong-Kuan Guo^{1,2,3‡}

¹*CAS Key Laboratory of Theoretical Physics,
Institute of Theoretical Physics, Chinese Academy of Sciences,
P.O. Box 2735, Beijing 100190, China*

²*School of Physical Sciences, University of Chinese Academy of Sciences,
No.19A Yuquan Road, Beijing 100049, China and*

³*School of Fundamental Physics and Mathematical Sciences,
Hangzhou Institute for Advanced Study,
University of Chinese Academy of Sciences, Hangzhou 310024, China*

Abstract

Space-based gravitational-wave detectors consist of a triangle of three spacecraft, which makes it possible to detect polarization modes of gravitational waves due to the motion of the detectors in space. In this paper we explore the ability of Taiji to detect the polarization modes in the parameterized post-Einsteinian framework. Assuming massive black hole binaries with the total mass of $M = 4 \times 10^5 M_\odot$ at redshift of $z = 1$, we find that Taiji can measure the dipole and quadruple emission ($\Delta\alpha_D/\alpha_D$ and $\Delta\alpha_Q/\alpha_Q$) with the accuracy of up to $\sim 0.04\%$, the scalar transverse and longitudinal modes ($\Delta\alpha_B$ and $\Delta\alpha_L$) up to ~ 0.01 , and the vector modes ($\Delta\alpha_V$) up to ~ 0.0005 .

* liuchang@itp.ac.cn

† ruanwenhong@itp.ac.cn

‡ guozk@itp.ac.cn

I. INTRODUCTION

So far, general relativity (GR) has passed a large number of experiments from solar system and binary pulsars [1–3]. Recently, the direct detections of gravitational waves (GWs) with advanced LIGO allow us to test GR in strong-field regime [4, 5]. In GR, GWs contain only two transverse-traceless polarization modes [6]. However, in alternative theories of gravity, GWs can have up to six polarization modes [7, 8]. For example, in Brans-Dicke theory there exists one scalar polarization mode in addition to the two transverse-traceless modes of GR [9], while in $f(R)$ gravity there are two additional scalar polarization modes [10–13]. Einstein-Aether theory predicts the existence of scalar and vector polarization modes [14–16], while generalized tensor-vector-scalar theories, such as TeVeS theory, predict the existence of all 6 polarization modes [17]. Therefore, the probe of the additional polarization modes allows us to capture deviations from GR [18].

However, it is hard to detect the additional polarization modes with advanced LIGO because its two detectors are co-oriented [19]. The future ground-based detector network of advanced LIGO with advanced Virgo, KAGRA and LIGO India, has the ability of probing additional polarization modes [20–22]. In addition, the space-based GW detectors, such as LISA [23] and Taiji [24], consist of a triangle of three spacecraft in orbit around the Sun, which make it possible to detect the additional polarization modes of GWs due to the motion of the detectors in space [25, 26].

Massive black hole binaries (MBHBs) are one of the main targets of space-based GW observatories, which are expected to be detected with extremely high signal-to-noise ratios (SNRs). So, the main purpose of this paper is to investigate the potential constraints on additional polarization modes of GWs with Taiji using the inspiral phase of MBHBs. To make our analysis model-independent, we use the parameterized post-Einsteinian (ppE) formalism, developed in Refs. [27, 28] to parameterize the effects on the non-GR polarization modes in modified gravity theories.

The paper is organized as follows. In Section II, we describe the leading order time-domain ppE waveforms for MBHBs. In Section III, the response signal of Taiji is obtained by using the rigid adiabatic approximation. In Section IV, we calculate the root-mean-

square errors of the ppE parameters by using the Fisher-matrix method. The last section is devoted to conclusions. Throughout this paper, we use units with $G = c = 1$, where G is the gravitational constant and c is the speed of light.

II. PARAMETERIZED POST-EINSTEINIAN WAVEFORM

In general, GWs have six polarization modes: two transverse-traceless modes, plus (+) and cross (\times), two vector longitudinal modes (U and V), a scalar transverse breathing mode (B), and a scalar longitudinal mode (L). The wave tensor with all six polarization modes can be written as

$$\mathbf{H}(t) = h_+(t)\boldsymbol{\epsilon}^+ + h_\times(t)\boldsymbol{\epsilon}^\times + h_U(t)\boldsymbol{\epsilon}^U + h_V(t)\boldsymbol{\epsilon}^V + h_B(t)\boldsymbol{\epsilon}^B + h_L(t)\boldsymbol{\epsilon}^L, \quad (1)$$

where $\boldsymbol{\epsilon}^A$ ($A = +, \times, U, V, B, L$) are the polarization tensors and h_A are the waveforms of the polarization modes. Following [29] we work in the heliocentric right-handed orthogonal reference frame $(\hat{x}, \hat{y}, \hat{z})$. In such a frame, the Sun is located at the origin of the coordinates, the x -axis is in the direction of vernal equinox, and the z -axis is parallel to the orbital angular momentum of the Earth. For a GW propagating in the \hat{k} direction, the bases of the source reference frame can be written as

$$\begin{aligned} \hat{k} &= -\sin\theta \cos\phi \hat{x} - \sin\theta \sin\phi \hat{y} - \cos\theta \hat{z}, \\ \hat{u} &= \cos\theta \cos\phi \hat{x} + \cos\theta \sin\phi \hat{y} - \sin\theta \hat{z}, \\ \hat{v} &= \sin\phi \hat{x} - \cos\phi \hat{y}, \end{aligned} \quad (2)$$

where (θ, ϕ) is the sky location of the source on the celestial sphere. Then the polarization tensors in (1) are given by

$$\begin{aligned} \boldsymbol{\epsilon}^+ &= \mathbf{e}^+ \cos 2\psi - \mathbf{e}^\times \sin 2\psi, \\ \boldsymbol{\epsilon}^\times &= \mathbf{e}^+ \sin 2\psi + \mathbf{e}^\times \cos 2\psi, \\ \boldsymbol{\epsilon}^U &= \mathbf{e}^U \cos \psi - \mathbf{e}^V \sin \psi, \\ \boldsymbol{\epsilon}^V &= \mathbf{e}^U \sin \psi + \mathbf{e}^V \cos \psi, \\ \boldsymbol{\epsilon}^B &= \mathbf{e}^B, \\ \boldsymbol{\epsilon}^L &= \mathbf{e}^L, \end{aligned} \quad (3)$$

where ψ is the polarization angle and the six basis tensors are [7]

$$\begin{aligned}
\mathbf{e}^+ &= \hat{u} \otimes \hat{u} - \hat{v} \otimes \hat{v}, \\
\mathbf{e}^\times &= \hat{u} \otimes \hat{v} + \hat{v} \otimes \hat{u}, \\
\mathbf{e}^U &= \hat{u} \otimes \hat{k} + \hat{k} \otimes \hat{u}, \\
\mathbf{e}^V &= \hat{v} \otimes \hat{k} + \hat{k} \otimes \hat{v}, \\
\mathbf{e}^B &= \hat{u} \otimes \hat{u} + \hat{v} \otimes \hat{v}, \\
\mathbf{e}^L &= \hat{k} \otimes \hat{k}.
\end{aligned} \tag{4}$$

Following Refs. [28, 30, 31], to leading order the waveforms in the ppE framework are

$$\begin{aligned}
h_+ &= \frac{2\mathcal{M}}{d_L} (\mathcal{M}\omega)^{2/3} (1 + \cos^2 \iota) \cos(2\Phi + 2\Phi_0), \\
h_\times &= \frac{4\mathcal{M}}{d_L} (\mathcal{M}\omega)^{2/3} \cos \iota \sin(2\Phi + 2\Phi_0), \\
h_U &= \frac{\alpha_V \mathcal{M}}{d_L} (\mathcal{M}\omega)^{1/3} \cos \iota \cos(\Phi + \Phi_0), \\
h_V &= \frac{\alpha_V \mathcal{M}}{d_L} (\mathcal{M}\omega)^{1/3} \sin(\Phi + \Phi_0), \\
h_B &= \frac{\alpha_B \mathcal{M}}{d_L} (\mathcal{M}\omega)^{1/3} \sin \iota \cos(\Phi + \Phi_0), \\
h_L &= \frac{\alpha_L \mathcal{M}}{d_L} (\mathcal{M}\omega)^{1/3} \sin \iota \cos(\Phi + \Phi_0),
\end{aligned} \tag{5}$$

where α_V , α_B , α_L are the dimensionless ppE parameters, d_L is the luminosity distance, $\mathcal{M} = M\eta^{3/5}$ is the chirp mass with the symmetric mass ratio $\eta = m_1 m_2 / M^2$ and the total mass $M = m_1 + m_2$, ι is the inclination angle, Φ is the orbital phase of the binary, and Φ_0 is the initial orbital phase. The evolution of orbital angular frequency is given by [31]

$$\frac{d\omega}{dt} = \alpha_D \eta^{2/5} \mathcal{M} \omega^3 + \alpha_Q \mathcal{M}^{5/3} \omega^{11/3}, \tag{6}$$

where α_D and α_Q characterize the dipole and quadrupole contribution to the frequency evolution respectively. To make our analysis independent of a specific model, we treat the ppE parameters $(\alpha_D, \alpha_Q, \alpha_V, \alpha_B, \alpha_L)$ as independent. In the GR case, $\alpha_D = \alpha_V = \alpha_B = \alpha_L = 0$ and $\alpha_Q = 96/5$. From (6), we can see that there is a degeneracy between α_D and η . The higher-order waveforms in the ppE framework are required to break such a degeneracy.

Since Eq. (6) does not have an explicit solution for $\omega(t)$, we can get $t(\omega)$

$$\begin{aligned}
t &= t_0 + \int_{\omega_0}^{\omega(t)} \frac{d\omega}{\alpha_D \eta^{2/5} \mathcal{M} \omega^3 + \alpha_Q \mathcal{M}^{5/3} \omega^{11/3}} \\
&= t_0 - \frac{(\omega^{-2} - \omega_0^{-2})}{2\mathcal{M}\eta^{2/5}\alpha_D} - \frac{3\alpha_Q^2 \mathcal{M}^{1/3}}{2\eta^{6/5}\alpha_D^3} \left(\frac{1}{\omega^{2/3}} - \frac{1}{\omega_0^{2/3}} \right) + \frac{3\alpha_Q \mathcal{M}^{-1/3}}{4\eta^{4/5}\alpha_D^2} \left(\frac{1}{\omega^{4/3}} - \frac{1}{\omega_0^{4/3}} \right) \\
&\quad + \frac{3\mathcal{M}\alpha_Q^3}{2\eta^{8/5}\alpha_D^4} \log \left(\frac{\eta^{2/5}\omega^{-2/3}\alpha_D + \mathcal{M}^{2/3}\alpha_Q}{\eta^{2/5}\omega_0^{-2/3}\alpha_D + \mathcal{M}^{2/3}\alpha_Q} \right), \tag{7}
\end{aligned}$$

where $\omega_0 = \omega(t_0)$ is the initial orbital angular frequency. The orbital phase is

$$\begin{aligned}
\Phi(t) &= \Phi_0 + \int_{t_0}^t \omega(t) dt \\
&= \Phi_0 + \int_{\omega_0}^{\omega(t)} \frac{\omega d\omega}{\alpha_D \eta^{2/5} \mathcal{M} \omega^3 + \alpha_Q \mathcal{M}^{5/3} \omega^{11/3}} \\
&= \Phi_0 - \frac{(\omega^{-1} - \omega_0^{-1})}{\alpha_D \eta^{2/5} \mathcal{M}} + \frac{3\alpha_Q \mathcal{M}^{-1/3}}{\alpha_D^2 \eta^{4/5}} \left(\frac{1}{\omega^{1/3}} - \frac{1}{\omega_0^{1/3}} \right) \\
&\quad + \frac{3\alpha_Q^{3/2}}{\alpha_D^{5/2} \eta} \left(\tan^{-1} \left(\frac{\sqrt{\alpha_Q} (\mathcal{M} \omega)^{1/3}}{\sqrt{\alpha_D} \eta^{1/5}} \right) - \tan^{-1} \left(\frac{\sqrt{\alpha_Q} (\mathcal{M} \omega_0)^{1/3}}{\sqrt{\alpha_D} \eta^{1/5}} \right) \right), \tag{8}
\end{aligned}$$

where $\Phi_0 = \Phi(t_0)$ is the initial orbital phase.

III. METHOD

For space-based GW detectors such as LISA and Taiji, the motion of the spacecraft in orbit around the Sun will introduce multiple modulations on the GW signals. In what follows we focus on Taiji. Under the rigid adiabatic approximation [29], the Michelson output with the spacecraft 1 as a synthesized detector can be written as

$$h(t) = \Re(\mathbf{F}(t, f(\xi)) : \mathbf{H}(\xi)), \tag{9}$$

where \Re denotes the real part, $\mathbf{a} : \mathbf{b} = a^{\mu\nu} b_{\mu\nu}$, and

$$\mathbf{F}(t, f(\xi)) = \frac{1}{2} [(\hat{r}_{12}(t) \otimes \hat{r}_{12}(t)) \mathcal{T}(\hat{r}_{12}(t), f(\xi)) - (\hat{r}_{13}(t) \otimes \hat{r}_{13}(t)) \mathcal{T}(\hat{r}_{13}(t), f(\xi))]. \tag{10}$$

The transfer function is [29]

$$\begin{aligned}
\mathcal{T}(\hat{r}_{ij}(t), f(\xi)) &= \frac{1}{2} \left[\text{sinc} \left(\frac{f(\xi)}{2f_*} (1 - \hat{r}_{ij}(t) \cdot \hat{k}) \right) \exp \left(-i \frac{f(\xi)}{2f_*} (3 + \hat{r}_{ij}(t) \cdot \hat{k}) \right) \right. \\
&\quad \left. + \text{sinc} \left(\frac{f(\xi)}{2f_*} (1 + \hat{r}_{ij}(t) \cdot \hat{k}) \right) \exp \left(-i \frac{f(\xi)}{2f_*} (1 + \hat{r}_{ij}(t) \cdot \hat{k}) \right) \right], \tag{11}
\end{aligned}$$

where $\text{sinc}(x) \equiv \sin(x)/x$, $\xi(t) = t - \hat{k} \cdot \mathbf{x}(t)$, and $f_* = 1/(2\pi L)$ with the arm-length of Taiji $L = 3 \times 10^9$ m. The coordinates $\mathbf{x}(t)$ of the three spacecraft in the heliocentric reference frame is given by [29]

$$\begin{aligned} x(t) &= R \cos \alpha + \frac{1}{2}eR [\cos(2\alpha - \beta) - 3 \cos \beta], \\ y(t) &= R \sin \alpha + \frac{1}{2}eR [\sin(2\alpha - \beta) - 3 \sin \beta], \\ z(t) &= -\sqrt{3}eR \cos(\alpha - \beta), \end{aligned} \quad (12)$$

where $R = 1$ AU, $e = L/(2\sqrt{3}R)$ is the orbit eccentricity, $\alpha = 2\pi f_m t + \kappa$ with $f_m = 1/\text{year}$, and $\beta = 2\pi n/3 + \lambda$ ($n = 0, 1, 2$). Here κ and λ are the initial ecliptic longitude and orientation of the spacecraft, respectively. The direction from the spacecraft i to the spacecraft j is described by

$$\hat{r}_{ij}(t) = \frac{\mathbf{x}_j(t) - \mathbf{x}_i(t)}{L}. \quad (13)$$

With the time-domain signal $h(t)$, we can get the Fourier transform of the signal by using the stationary phase approximation [32]. The GW parameters in the ppE framework is

$$\boldsymbol{\lambda} = \{t_c, \Phi_0, \theta, \phi, \psi, \iota, \mathcal{M}, d_L, \alpha_D, \alpha_Q, \alpha_V, \alpha_B, \alpha_L\}. \quad (14)$$

We use the Fisher-matrix method to explore the ability of Taiji to detect deviations from GR. The method is based on computing the inverse of the Fisher matrix, known as the variance-covariance matrix. The diagonal elements of the variance-covariance matrix are maximum likelihood estimators of the variance of parameters around the true value in the case of a large SNR [33].

The Fisher information matrix is defined as

$$\Gamma_{ij} \equiv \left(\frac{\partial h}{\partial \lambda_i}, \frac{\partial h}{\partial \lambda_j} \right), \quad (15)$$

where the noise-weighted inner product is

$$(a, b) = 2 \int_0^\infty df \frac{\tilde{a}(f)\tilde{b}^*(f) + \tilde{a}^*(f)\tilde{b}(f)}{S_n(f)}. \quad (16)$$

Here $S_n(f)$ is the noise power spectral density of Taiji [34–36]. If the noise is Gaussian and stationary, the root-mean-square error in λ_i is

$$\Delta\lambda_i = \sqrt{(\Gamma^{-1})_{ii}}, \quad (17)$$

where Γ^{-1} is the inverse of the Fisher matrix. In our analysis, we use two Michelson channels and the combined Fisher matrix is a sum of two Fisher matrices.

IV. RESULTS

To investigate the ability of Taiji to detect the additional polarization modes, we focus on the parameter estimation of the five ppE parameters ($\alpha_D, \alpha_Q, \alpha_B, \alpha_V, \alpha_L$) with the fiducial values of $\alpha_D = 0.001$ ¹, $\alpha_Q = 19.2$, $\alpha_V = 0$, $\alpha_B = 0$ and $\alpha_L = 0$. We consider equal-mass MBHBs with the total mass of $M = 4 \times 10^5 M_\odot$ in the source frame at redshift of $z = 1$. The corresponding luminosity distance can be calculated in a spatially-flat Λ CDM Universe with the matter density parameter $\Omega_m = 0.3$ and Hubble constant $H_0 = 67 \text{ km s}^{-1} \text{ Mpc}^{-1}$. We consider only the inspiral phase of MBHBs, neglecting all information coming from the merger and the ringdown phases. In our analysis the coalescence time is chosen to be 60 days which means the inspiral is observed for 60 days before it reaches the innermost stable circular orbit.

A. Inclination angle

Setting $\theta = \pi/4$, $\phi = \pi$ and $\psi = 0.1$, we generate 50 equal-mass MBHBs with the inclination angle from $\iota = 0$ to π . Fig. 1 shows the errors in the five ppE parameters and SNRs as a function of the inclination angle.

From Fig. 1 we see that the measurements of α_D , α_Q and α_V are better when $\iota = 0$ or π (face-on) with larger SNRs than the case of $\iota = \pi/2$ (edge-on). However, the measurement errors in α_B and α_L increase when the inclination angle approaches to 0 or π . This is because that the $\sin \iota$ dependence of the waveforms in Eq. (5) implies that for the scalar modes (B and L), the signal for the edge-on binary is stronger than the face-on binary. Actually, in the heliocentric frame, the signals contain the effects of the relative orientation and motion of the sources and the detectors by the response functions. Therefore, the errors in α_B and α_L have a local maximum at $\iota \sim \pi/2$, as shown in the top-right panel of Fig. 1. Our further

¹ Although α_D vanishes in GR, in our analysis $\alpha_D = 0.001$ is chosen to avoid the divergence of (7) and (8).

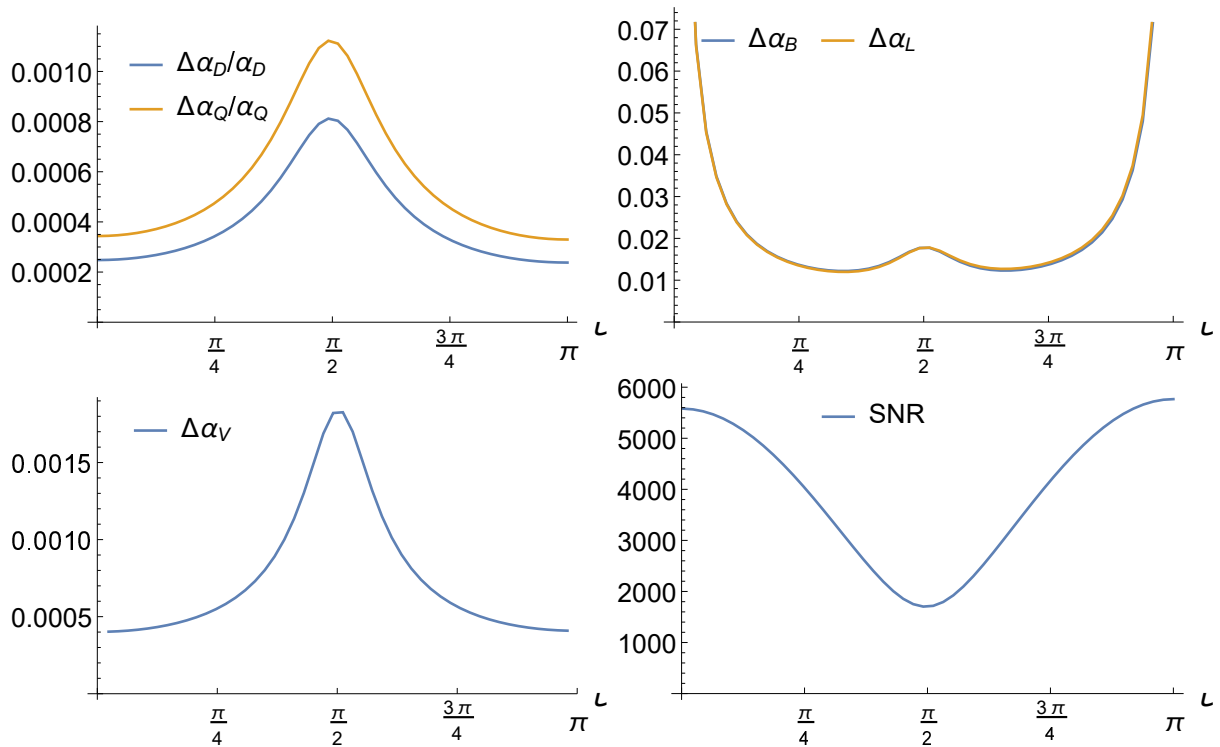


FIG. 1. Errors in the five ppE parameters and SNRs as a function of the inclination angle for equal-mass MBHBs with the total mass of $M = 5 \times 10^5 M_\odot$ at redshift of $z = 1$.

calculations indicate that the local maximum disappears for sources with some special sky locations. Since the fiducial values of the five ppE parameters are chosen in GR with only the + and \times modes, as expected, the SNR for the face-on binary is larger than the edge-on one. With Taiji, $\Delta\alpha_D/\alpha_D$ and $\Delta\alpha_Q/\alpha_Q$ can be measured with the accuracy of up to $\sim 0.04\%$, $\Delta\alpha_B$ and $\Delta\alpha_L$ up to ~ 0.01 , and $\Delta\alpha_V$ up to ~ 0.0005 .

B. Polarization angle

We generate 50 equal-mass MBHB sources in the range of $0 < \psi < \pi$, with the fixed values of $\theta = \pi/4$, $\phi = \pi$ and $\iota = \pi/4$. Fig. 2 shows the errors in the five ppE parameters and SNRs as a function of the polarization angle.

The errors in α_B , α_L and α_V vary with a period of π , while the errors in α_D and α_Q and SNRs vary with a period of $\pi/2$, as shown in Fig. 2. Moreover, the errors in α_D and α_Q

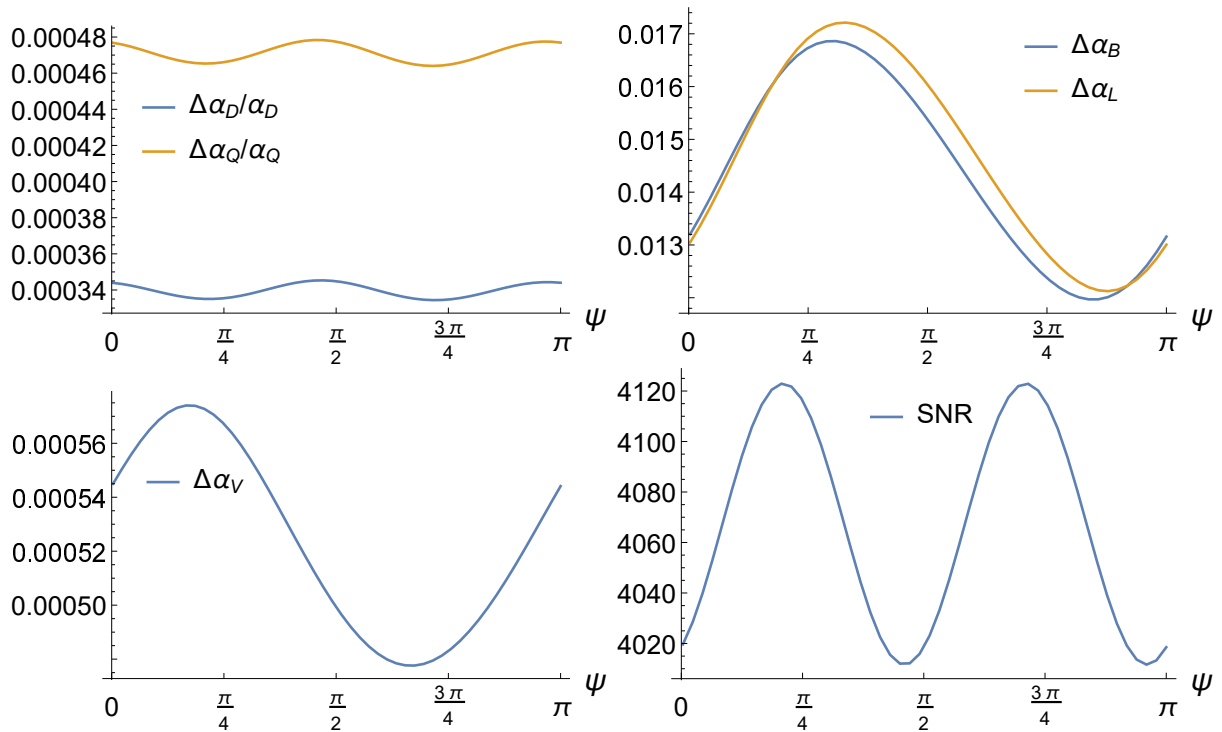


FIG. 2. Errors in the five ppE parameters and SNRs as a function of the polarization angle.

decrease when the SNRs increase as a function of the polarization angle.

C. Sky location

Assuming $\iota = \pi/4$ and $\psi = 0.1$, we generate 400 equal-mass MBHB sources with different sky locations ($0 < \theta < \pi$, $0 < \phi < 2\pi$) to illustrate the sky-location dependence of the errors in the five ppE parameters and SNRs in Fig. 3.

We find the errors in α_D and α_Q become small for large SNRs as a function of the sky location. This is the case as a function of the inclination angle in Subsections IV A and as a function of the polarization angle in Subsections IV B. However, for the other three ppE parameters, α_B , α_L and α_V , the parameter errors become large for large SNRs as a function of the sky location. Since the fiducial values of the ppE parameters are chosen in GR, as expected, the sky-location dependence of the SNRs is consistent with the result of LISA [37]. Note that the parameter errors and SNRs are predominantly axisymmetric.

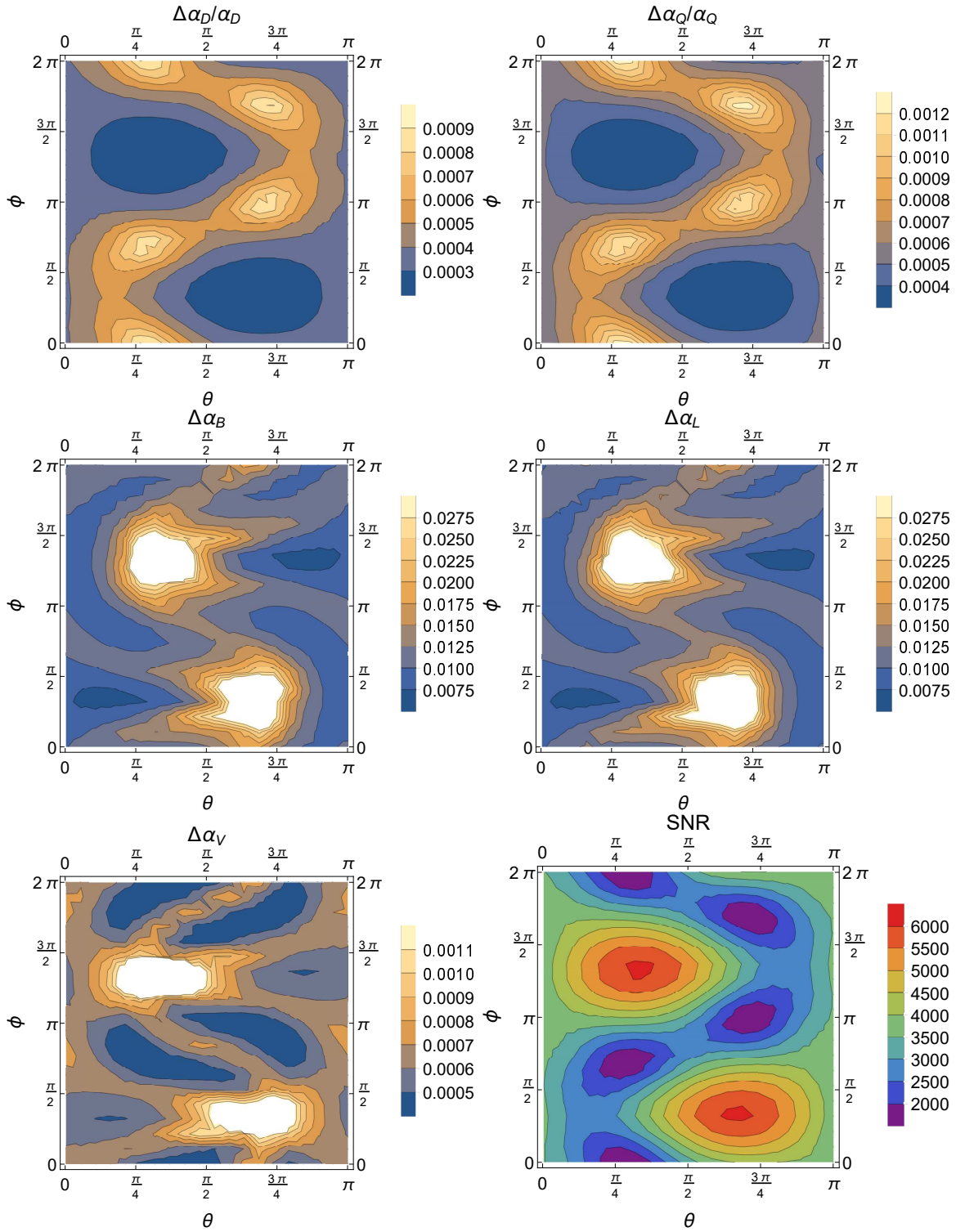


FIG. 3. Sky-location dependence of the errors in the five ppE parameters and SNRs.

V. CONCLUSIONS

We have investigated the ability of Taiji to detect the additional polarization modes of GWs by using the ppE waveforms for the inspiral phase of MBHBs. The Fisher-matrix method is used to compute the parameter errors in the five ppE parameters, α_D , α_Q , α_B , α_V and α_L . In our analysis, the fiducial values of the ppE parameters are set in the GR case. The coalescence time is chosen to be 60 days for equal-mass MBHBs with the total mass of $M = 4 \times 10^5 M_\odot$ at redshift of $z = 1$. Moreover, we have studied the behavior of the parameter errors as functions of the inclination angle, polarization angle and direction to the binary, respectively.

The behavior of $\Delta\alpha_D/\alpha_D$ is the same as that of $\Delta\alpha_Q/\alpha_Q$ as functions of ι , ψ and the sky location. Both $\Delta\alpha_D/\alpha_D$ and $\Delta\alpha_Q/\alpha_Q$ become small for large SNRs, which can be measured with the accuracy of up to $\sim 0.04\%$. Although the waveforms of the scalar transverse and longitudinal modes in the ppE framework are the same in Eq. (5), the polarization tensors and response functions help us to break their degeneracy. The behavior of $\Delta\alpha_B$ is similar to that of $\Delta\alpha_L$ as functions of the inclination angle, polarization angle and sky location. The measurement accuracy of up to 0.01 can be achieved. Compared to the scalar polarization modes, GWs in the inspiral phase of MBHBs are sensitive to the vector polarization modes, which is measured with the accuracy of up to 0.0005.

ACKNOWLEDGMENTS

This work is supported in part by the National Natural Science Foundation of China Grants No. 11690021 and No. 11851302, in part by the Strategic Priority Research Program of the Chinese Academy of Sciences Grants No. XDB23030100 and No. XDA15020701, and by Key Research Program of Frontier Sciences, CAS.

-
- [1] I. H. Stairs, Living Rev. Rel. **6**, 5 (2003) [astro-ph/0307536].
 - [2] C. M. Will, Living Rev. Rel. **17**, 4 (2014) [arXiv:1403.7377 [gr-qc]].

- [3] N. Wex, [arXiv:1402.5594 [gr-qc]].
- [4] B. Abbott *et al.* [LIGO Scientific and Virgo], Phys. Rev. Lett. **116**, no.6, 061102 (2016) [arXiv:1602.03837 [gr-qc]].
- [5] B. Abbott *et al.* [LIGO Scientific and Virgo], Phys. Rev. D **100**, no.10, 104036 (2019) [arXiv:1903.04467 [gr-qc]].
- [6] D. Eardley, D. Lee and A. Lightman, Phys. Rev. D **8**, 3308-3321 (1973)
- [7] A. Nishizawa, A. Taruya, K. Hayama, S. Kawamura and M. a. Sakagami, Phys. Rev. D **79**, 082002 (2009) [arXiv:0903.0528 [astro-ph.CO]].
- [8] Y. Gong and S. Hou, Universe **4**, no.8, 85 (2018) [arXiv:1806.04027 [gr-qc]].
- [9] C. Brans and R. Dicke, Phys. Rev. **124**, 925-935 (1961)
- [10] M. E. Alves, O. D. Miranda and J. C. de Araujo, Phys. Lett. B **679**, 401-406 (2009) [arXiv:0908.0861 [gr-qc]].
- [11] A. De Felice and S. Tsujikawa, Living Rev. Rel. **13**, 3 (2010) [arXiv:1002.4928 [gr-qc]].
- [12] H. Rizwana Kausar, L. Philippoz and P. Jetzer, Phys. Rev. D **93**, no.12, 124071 (2016) [arXiv:1606.07000 [gr-qc]].
- [13] D. Liang, Y. Gong, S. Hou and Y. Liu, Phys. Rev. D **95**, no.10, 104034 (2017) [arXiv:1701.05998 [gr-qc]].
- [14] T. Jacobson and D. Mattingly, Phys. Rev. D **70**, 024003 (2004) [arXiv:gr-qc/0402005 [gr-qc]].
- [15] K. Lin, X. Zhao, C. Zhang, T. Liu, B. Wang, S. Zhang, X. Zhang, W. Zhao, T. Zhu and A. Wang, Phys. Rev. D **99**, no.2, 023010 (2019) [arXiv:1810.07707 [astro-ph.GA]].
- [16] C. Zhang, X. Zhao, A. Wang, B. Wang, K. Yagi, N. Yunes, W. Zhao and T. Zhu, Phys. Rev. D **101**, no.4, 044002 (2020) [arXiv:1911.10278 [gr-qc]].
- [17] J. D. Bekenstein, Phys. Rev. D **70**, 083509 (2004) [arXiv:astro-ph/0403694 [astro-ph]].
- [18] B. P. Abbott *et al.* [LIGO Scientific and Virgo], Phys. Rev. Lett. **120**, no.20, 201102 (2018) [arXiv:1802.10194 [gr-qc]].
- [19] M. Isi and A. J. Weinstein, [arXiv:1710.03794 [gr-qc]].
- [20] N. Yunes and X. Siemens, Living Rev. Rel. **16**, 9 (2013) [arXiv:1304.3473 [gr-qc]].
- [21] Y. Hagihara, N. Era, D. Iikawa, A. Nishizawa and H. Asada, Phys. Rev. D **100**, no.6, 064010 (2019) [arXiv:1904.02300 [gr-qc]].

- [22] H. Takeda, A. Nishizawa, K. Nagano, Y. Michimura, K. Komori, M. Ando and K. Hayama, Phys. Rev. D **100**, no.4, 042001 (2019) [arXiv:1904.09989 [gr-qc]].
- [23] P. Amaro-Seoane *et al.* [LISA], [arXiv:1702.00786 [astro-ph.IM]].
- [24] W. R. Hu and Y. L. Wu, Natl. Sci. Rev. **4**, no.5, 685-686 (2017)
- [25] J. R. Gair, M. Vallisneri, S. L. Larson and J. G. Baker, Living Rev. Rel. **16**, 7 (2013) [arXiv:1212.5575 [gr-qc]].
- [26] L. Philippoz and P. Jetzer, J. Phys. Conf. Ser. **840**, no.1, 012057 (2017)
- [27] N. Yunes and F. Pretorius, Phys. Rev. D **80**, 122003 (2009) [arXiv:0909.3328 [gr-qc]].
- [28] K. Chatziioannou, N. Yunes and N. Cornish, Phys. Rev. D **86**, 022004 (2012) [arXiv:1204.2585 [gr-qc]].
- [29] L. J. Rubbo, N. J. Cornish and O. Poujade, Phys. Rev. D **69**, 082003 (2004) [arXiv:gr-qc/0311069 [gr-qc]].
- [30] D. Hansen, N. Yunes and K. Yagi, Phys. Rev. D **91**, no.8, 082003 (2015) [arXiv:1412.4132 [gr-qc]].
- [31] L. O’Beirne, N. J. Cornish, S. J. Vigeland and S. R. Taylor, Phys. Rev. D **99**, no.12, 124039 (2019) [arXiv:1904.02744 [gr-qc]].
- [32] N. Yunes, K. Arun, E. Berti and C. M. Will, Phys. Rev. D **80**, no.8, 084001 (2009) [arXiv:0906.0313 [gr-qc]].
- [33] M. Vallisneri, Phys. Rev. D **77**, 042001 (2008) [arXiv:gr-qc/0703086 [gr-qc]].
- [34] W. H. Ruan, Z. K. Guo, R. G. Cai and Y. Z. Zhang, Int. J. Mod. Phys. A **35**, 2050075 (2020) [arXiv:1807.09495 [gr-qc]].
- [35] W. H. Ruan, C. Liu, Z. K. Guo, Y. L. Wu and R. G. Cai, [arXiv:1909.07104 [gr-qc]].
- [36] W. H. Ruan, C. Liu, Z. K. Guo, Y. L. Wu and R. G. Cai, Nat. Astron. **4**, 108-109 (2020) [arXiv:2002.03603 [gr-qc]].
- [37] T. Robson, N. J. Cornish and C. Liu, Class. Quant. Grav. **36**, no.10, 105011 (2019) [arXiv:1803.01944 [astro-ph.HE]].